Plant Physiol. (1990) 94, 926–934
0032-0889/90/94/0926/09/$01.00/0

Received for publication April 18, 1990
Accepted June 19, 1990

Photoacoustic Measurements *in Vivo* of Energy Storage by Cyclic Electron Flow in Algae and Higher Plants[1]

Stephen K. Herbert, David C. Fork*, and Shmuel Malkin[2]

Carnegie Institution of Washington, Department of Plant Biology, Stanford, California 94305

ABSTRACT

Energy storage by cyclic electron flow through photosystem I (PSI) was measured *in vivo* using the photoacoustic technique. A wide variety of photosynthetic organisms were considered and all showed measurable energy storage by PSI-cyclic electron flow except for higher plants using the C-3 carbon fixation pathway. The capacity for energy storage by PSI-cyclic electron flow alone was found to be small in comparison to that of linear and cyclic electron flows combined but may be significant, nonetheless, under conditions when photosystem II is damaged, particularly in cyanobacteria. Light-induced dynamics of energy storage by PSI-cyclic electron flow were evident, demonstrating regulation under changing environmental conditions.

The oxygen-evolving photosynthetic apparatus contains two reaction center complexes, designated PSI and PSII, which convert light to electrochemical potential and function in series to drive a linear flow of electrons from H_2O to $NADP^+$, producing O_2 as a by-product. This linear electron flow also produces a proton gradient across the photosynthetic thylakoid membrane that is utilized to phosphorylate ADP.

In addition to linear electron flow, other patterns of electron flow occur in oxygen-evolving photosynthesis that have various functions. The most significant nonlinear pattern of electron flow, in terms of converting light to useful electrochemical potential, is the cyclic flow of electrons through PSI that also contributes to the *trans*-thylakoid proton gradient and, thereby, to the synthesis of ATP. In the photosynthetic bacteria that do not evolve oxygen, some form of cyclic electron flow through a PSI analog is the primary means by which light is utilized.

In oxygen-evolving phototrophs, the physiological significance of cyclic electron flow through PSI is uncertain. A clearly defined role for cyclic electron flow through PSI has been established in higher plants having the C_4 carbon fixation pathway (21), but no such clear role has been determined in plants having the more common C_3 carbon fixation pathway. Myers (20) studied the steady-state poise of P700 and the rate of photoreaction I in three cyanobacteria and reached the 'monstrous' conclusion that cyclic electron flow is not a significant process in these organisms. Traditionally, cyclic electron flow through PSI in C_3 plants has been proposed to generate ATP over and above that produced by linear electron flow, adjusting the ratio of ATP to NADPH generated by the light reactions of photosynthesis in accordance with the needs of the plant (1). As an example, cyclic electron flow through PSI has been proposed as a source of ATP for repair of PSII units damaged by environmental stress, since PSI is typically much less susceptible to stress than PSII (8, 9).

Much of the ambiguity concerning the function and significance of cyclic electron flow through PSI is due to the difficulty of measuring it in whole cells and tissues. Most previous studies of PSI-cyclic electron flow and accompanying phosphorylation have necessarily used either *in vitro* measurements of thylakoid fragments or somewhat ambiguous light-induced absorbance changes in whole cells or tissues (12, 17). The photoacoustic method for measurement of photosynthetic energy storage is well suited for study of PSI-cyclic electron flow, however, because it is capable of simple, direct, and quantitative measurement of energy storage by cyclic electron flow in intact leaves and algae as well as in thylakoid preparations (9, 10, 16, 18). Presumably, the bulk of such energy storage by PSI-cyclic electron flow represents photophosphorylation of ADP.

In the present report, the occurrence, capacity, and regulation of energy storage by PSI-cyclic electron flow in whole tissues of a variety of photosynthetic organisms are characterized using the photoacoustic method.

MATERIALS AND METHODS

Plant Material

Specimens of *Porphyra perforata* J. Agardh (Rhodophyta), *Macrocystis pyrifera* (L.) C. Agardh (Chromophyta), and *Ulva* sp. (Chlorophyta) were collected from beaches in San Mateo County, CA, and cultured under vigorous aeration in Guillard's f/2 enriched seawater medium changed twice weekly. Lighting was by cool-white fluorescent tubes at 25 μmol photons m^{-2} s^{-1} (400–700 nm), photoperiod was 12 h light:12 h dark and temperature was 15°C. These plants were used for experiments after 1 to 3 weeks of acclimation to culture conditions. The cyanobacterium *Anacystis nidulans,* strain R2, was grown in aerated culture tubes in Allen's BG-11 medium at 29°C and 50 μmol photons m^{-2} s^{-1} continuous light from incandescent bulbs. Measurements were made on these cells during the log phase of population growth.

Samples of *Oxalis corniculata* L. were collected from the grounds of the Carnegie Institution and samples of *Sorghum*

[1] Carnegie Institution of Washington, Department of Plant Biology Publication No. 1075.

[2] Present address: The Weizmann Institute of Science, Rehovot, Israel.

bicolor L. were obtained from plants grown in the Carnegie glasshouses.

Photoacoustic Energy Storage Measurements

The yield of photosynthetic ES[3] was measured using the photoacoustic technique. This technique is described in detail elsewhere (5, 6). In brief, thermal photoacoustic signals are used to quantify the conversion of absorbed light to heat in a sample. If the sample is not performing photochemistry, the conversion is 100%. If, however, some of the light energy is being stored as products of photochemistry, as in the case of a leaf or algal sample performing photosynthesis, it is unavailable for conversion to heat and its absence from the thermal photoacoustic signal can be quantified. Modulated oxygen evolution from photosynthetic samples also produces a photoacoustic signal but in the present study the oxygen component of the signal was absent and only the thermal signal was considered (see below).

The photoacoustic apparatus used was similar to that described elsewhere (18). Modulated measuring light was produced with an optical chopper (Stanford Research Systems model SR540) used in conjunction with a xenon arc lamp (ILC R300-3) and monochromator (Bausch and Lomb). Intensity of the modulated light was controlled by neutral density filters and by varying the slit width of the monochromator. Nonmodulated background light was from a quartz-iodine incandescent lamp (General Electric type EJM) and was also passed through Calflex C heat-reflecting filter. Modulated and background lights were focused onto the branches of a bifurcated fiber-optic cable that delivered light to the photoacoustic cell. The photoacoustic cell was a small acrylic plastic chamber (about 0.1 mL volume) which communicated with a tiny microphone (Knowles Electronics, type 1785) through a small channel. The relevant signal from the microphone was selected and amplified with a lock-in amplifier (Stanford Research Systems model SR-510) and recorded on a strip chart recorder (E and K Scientific Products).

Percent ES was calculated as $(a - b)/a \times 100$ where a was the photoacoustic signal produced by the modulated light during addition of nonmodulated background light of 1180 or 2000 μmol photons m^{-2} s^{-1} and b was the photoacoustic signal in the modulated light alone. Addition of strong background light acts to saturate photochemistry in the sample, increasing the conversion of the absorbed modulated light to heat to nearly 100% and producing a maximum photoacoustic signal proportional to absorption of the modulated light by the sample. In the presence of the modulated light alone, photochemistry is not saturated and a reduced photoacoustic signal is observed as a result of storage of a substantial part of the absorbed modulated light as products of photosynthesis. ES is thus a measure of the efficiency of photosynthetic photochemistry comparable to the quantum yield. It should be noted that the ES parameter has been referred to as photochemical loss (PL) in other publications.

For ES measurements, 1 cm discs of whole tissue were moistened and adhered to a glass slide that was then clamped against the o-ring seal of the photoacoustic chamber with a transparent backing plate so that the sample was inside the chamber. In the case of *Anacystis,* cells were filtered down onto a disc of membrane filter (Millipore, 0.45 μm pore size) which was then loaded into the chamber (7). The modulation frequency of the measuring light was adjusted for each sample type so that no oxygen signal was observed with the lock-in amplifier set at the quadrature phase angle (90° out of phase from the phase angle giving the maximum photoacoustic signal in the presence of strong background light). The phase angle was then rotated 90° to be in phase for the thermal signal during measurements. These precautions assured that the contribution of modulated oxygen evolution to the measured photoacoustic signal was negligibly small (9, 22). Higher plant leaves were vacuum-infiltrated with water to allow measurements of the thermal signal to be made at the relatively low frequency of 20 Hz.

Maximal ES values were measured at low measuring light intensity and were, therefore, proportional to the quantum yield of light-limited photosynthesis. Once sealed in the chamber, the samples maintained maximal ES values for hours with no obvious signs of fatigue or stress. If the intensity of the measuring light was increased, ES values declined as photosynthesis became light-saturated and quantum yield decreased. ES at high measuring beam intensities also showed a decline over time to a stable value as, presumably, CO_2 in the sealed photoacoustic cell was depleted to the level of the CO_2 compensation point. For this reason, our measurements of ES used to calculate ES capacity were made quickly (1–3 min) before apparent CO_2 limitation was observed to occur.

The temperature at which ES measurements were made was 20 to 23°C. Inhibitors were administered by soaking the samples in inhibitor solutions prior to loading the samples into the photoacoustic cell or, in the case of leaves, vacuum-infiltrating the leaves with inhibitor solutions. DBMIB was kept in the reduced form by adding 5 mM Na ascorbate to the solution.

RESULTS

Figure 1 shows photoacoustic signal tracings for representatives of higher plants and all the major groups of algae. With one exception, all groups showed measurable energy storage in narrowband, far red light absorbed almost exclusively by PSI. The notable exception was *Oxalis corniculata,* a higher plant using the C_3 carbon fixation pathway. In general, C_3 plants such as *Oxalis* and *Phaseolus vulgaris* did not show any photoacoustically measurable energy storage in far red light while C_4 plants, such as *Sorghum bicolor* and *Zea mays,* consistently showed easily measurable energy storage in far red light (data for plants other than *Oxalis* and *Sorghum* not shown).

Other features of interest are present in Figure 1. The traces for *Anacystis* and *Sorghum* show the effect of adding weak, nonmodulated background light absorbed by PSII to a far red measuring light. The weak PSII light enhanced energy storage by allowing PSI to participate in linear as well as cyclic electron flow (18). This enhancement effect was observed in all the plants shown in Figure 1 and was consistently abolished

[3] Abbreviations: ES, photoacoustically measured energy storage; DBMIB, 2,5-dibromo-3-methyl-6-isopropyl-*p*-benzoquinone; CCCP, carbonylcyanide *m*-chlorophenylhydrazone.

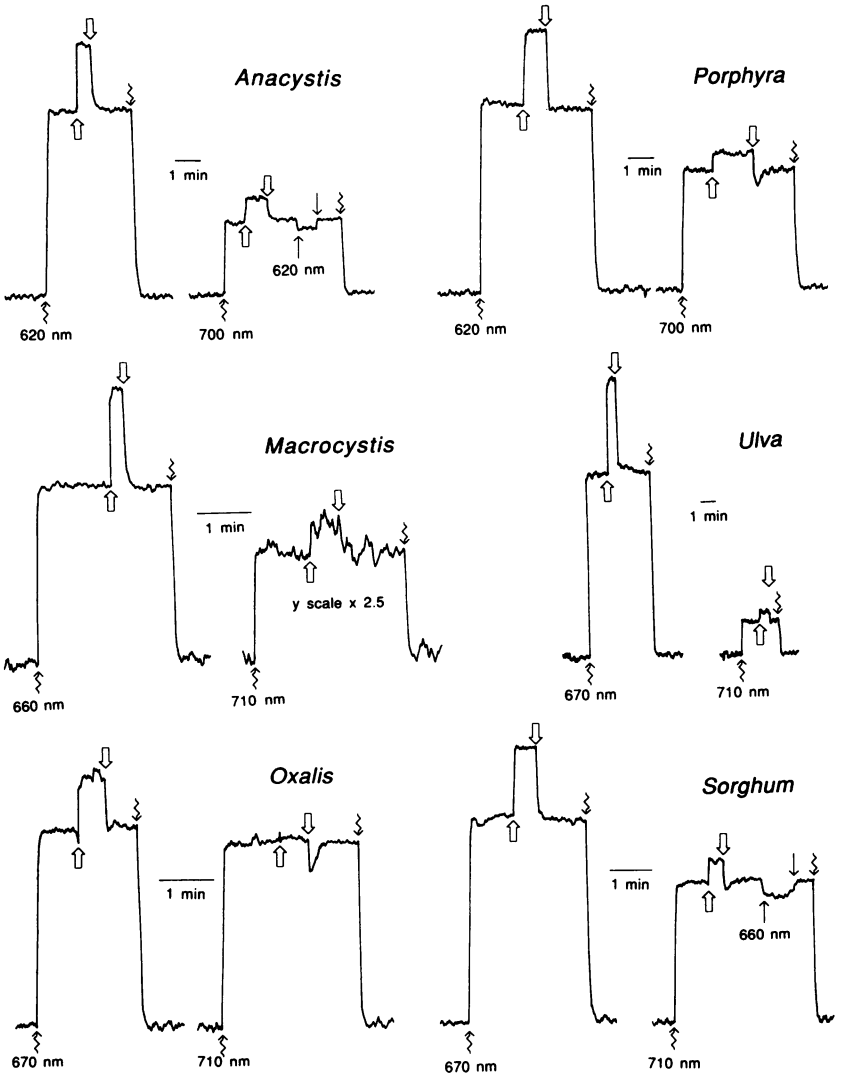

Figure 1. Photoacoustic signals in wavelengths of measuring light absorbed by both PSII and PSI (620–670 nm) or by PSI only (700–710 nm). Upward-pointing arrows indicate light on and downward-pointing arrows indicate light off. Thin wavy arrows represent the modulated measuring light (4.8 nm half-bandwidth), thin straight arrows represent weak nonmodulated background light (4.8 nm half-bandwidth), thick straight arrows represent strong nonmodulated background light (white). Average intensities of the modulated measuring light (expressed as μmol photons m^{-2} s^{-1}) were: 17.6 (620 nm), 26.5 (660 nm), 25.8 (670 nm *Ulva*) 17.4 (670 nm *Oxalis* and *Sorghum*), 15.8 (700 nm), 20.2 (710 nm *Ulva*), and 30.9 (710 nm *Oxalis* and *Sorghum*). Intensities of the weak nonmodulated background lights were 29.0 (620 nm) and 31.5 (660). Intensities of the strong, nonmodulated white background light (in the wavelength band 400–700 nm) were 2000 (*Ulva* and *Macrocystis*) and 1180 (all others). Modulation frequencies in Hz for the measuring light were 20 (*Porphyra, Oxalis, Sorghum*), 64 (*Ulva*), 95 (*Anacystis*), or 215 (*Macrocystis*). Leaves of *Oxalis* and *Sorghum* were vacuum-infiltrated with water to allow thermal signal measurement at 20 Hz without interference from an oxygen signal. The y-scale is relative between species but constant within species except for *Macrocystis*.

by DCMU (data not shown). Traces for *Porphyra, Oxalis,* and *Sorghum* in far red measuring light also showed a downward transient when strong, white, nonmodulated background light that had been added to a far red measuring light was turned off. This off-transient may represent momentary enhancement of energy storage by electrons from an intersystem pool of electron carriers that was reduced by the action of the strong white background light on PSII and then rapidly oxidized when the white light was turned off, causing the enhancement to reverse. These off-transients were also abolished by DCMU. The samples used for energy storage measurements were typically not dark-adapted so that dark to light transients were not usually seen when the measuring light was turned on. As a rule, ES measurements were made when the sample had achieved an apparent steady-state in the measuring light. The time required to achieve a steady-state varied from a few seconds to a minute or more, depending on the intensity of the measuring beam (faster at lower intensity).

The spectral response of energy storage in the presence and absence of DCMU is shown in Figure 2. Two precautions were taken in these measurements to assure that the energy storage values presented in the spectra were proportional to the quantum yield of photosynthesis. First, the intensity of the modulated measuring beam and its absorption by the sample varied somewhat from one wavelength to the next in these measurements but was kept well within the linear range of maximum ES for wavelengths less than 680 nm. Second, energy storage values were corrected by the factor 690 nm/λ where λ was the wavelength of the measuring light in nm. This factor corrected for the loss of energy that occurred as quanta of wavelengths shorter than 680 or 700 nm were utilized by the photosynthetic antennae to oxidize the reaction centers of PSI and PSII, respectively.

The spectra of Figure 2 show several consistent general features. Energy storage at wavelengths below 660 nm for *Porphyra* and *Anacystis* and below 680 nm for the other plants was relatively stable at close to maximal values. Beyond these two wavelengths, a clear 'red drop' was observed, mirroring the known response for the quantum yield of oxygen evolution (4). At wavelengths longer than the red drop, energy storage rose again to a peak at 700 to 710 nm in plants other than *Oxalis,* reminiscent of the 'red rise' described by Arnon

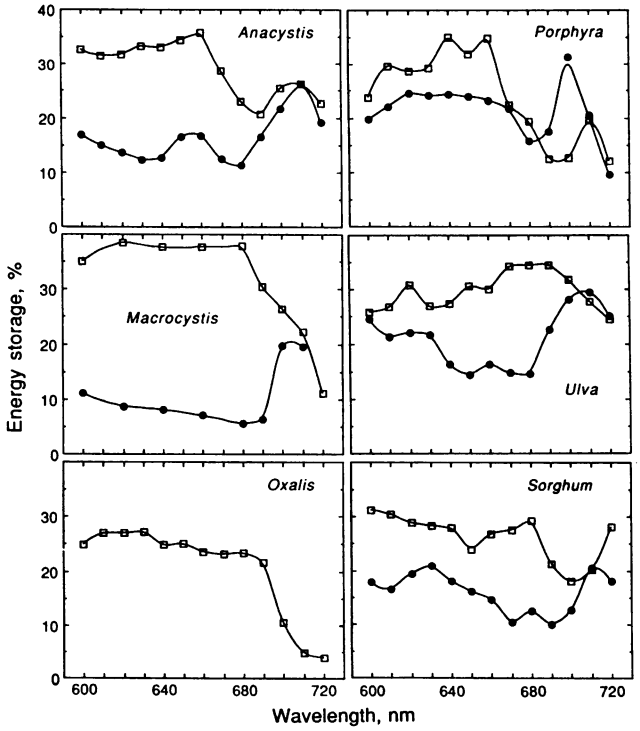

Figure 2. Spectral response of energy storage (ES) for controls (□) and for samples in 25 μM DCMU (●). Half-bandwidth of the monochromatic light was 4.8 nm. Modulation frequencies of the measuring light were the same for each species as in Figure 1. Intensities of the measuring light were well within the flat, maximal region of the ES *versus* measuring light intensity response for wavelengths of 680 nm and below in samples without DCMU. Nonmodulated white background light (in the wavelength band 400–700) was 1180 μmol photons m^{-2} s^{-1}. ES was calculated as described in "Materials and Methods" from traces like those of Figure 1.

for PSI-mediated phosphorylation produced by cyclic electron flow (1). The 700 to 710 nm far red peak was either unaffected or, in the case of *Porphyra,* improved by addition of 25 μM DCMU to the sample. Energy storage at wavelengths shorter than 700 nm was clearly inhibited by DCMU. In the case of *Oxalis,* energy storage in DCMU was not detectable.

The effects of DCMU, DBMIB, and CCCP on energy storage of far red light in *Porphyra* and *Ulva* are presented in Table I. These data show that while DCMU had a neutral or positive effect on energy storage in far red light, both DBMIB and CCCP inhibited such energy storage. DBMIB is a plastoquinone antagonist that inhibits cyclic and linear electron flow while CCCP is an uncoupler that inhibits cyclic photophosphorylation and secondarily inhibits water oxidation at high concentrations (15, 24). It should be noted that at concentrations of 100 μM, both DBMIB and CCCP strongly inhibited linear electron flow, measured polarographically as O_2 evolution, in both *Ulva* and *Porphyra* (data not shown). For *Porphyra,* therefore, DBMIB or CCCP treatments are best compared with the DCMU-treated ES value. *Porphyra* samples treated with DBMIB and DCMU together showed no measurable ES (data not shown).

ES *versus* absorbed measuring light is shown for *Ulva* in Figure 3. The values plotted on the *x*-axis are the maximum photoacoustic signal in the presence of the strong, nonmodulated white background light, which is proportional to the amount of modulated measuring light absorbed by the sample. The ES values of the *y*-axis have also been corrected by the factor 690 nm/λ. The 670 nm values in Figure 3 are typical of the ES *versus* intensity response (5), an initial flat region of maximal values at low intensity corresponding to truly light-limited photosynthesis and maximum quantum yield, followed by a descending curve of energy storage values as light intensity increases and photosynthesis becomes light-saturated. The 710 nm points in Figure 3 show only the descending curve. An initial flat region of maximal ES values in 710 nm measuring light, if present, was not observable in our measurements, suggesting that energy storage by PSI-cyclic electron flow became light-saturated at very low light intensities relative to energy storage by linear and cyclic flow combined. The results for the *Ulva* sample of Figure 3 were qualitatively typical of the other algal subjects of this study.

ES *versus* the average intensity of the modulated measuring light in the presence and absence of DCMU or DBMIB is shown for three algal species in Figure 4. The measuring light used for these experiments was narrowband, absorbed primarily by PSII, and the ES values were corrected by the factor 690 nm/λ. In the plots of Figure 4, only the flat, maximal region of energy storage is present in samples not treated with inhibitors. Like the 710 nm plot of Figure 3, a flat, maximal energy storage region was not observable in the presence of 25 μM DCMU and only a descending curve of energy storage with increasing light was seen. In 100 μM DBMIB, a similar response was observed but the ES values were significantly lower than for DCMU. These responses indicate that the effect of DCMU and DBMIB on energy storage in light absorbed by PSII was to dramatically reduce the capacity for energy storage and, thereby, to reduce the measuring light intensity at which energy storage begins to be light-saturated.

The energy storage capacity of a sample should be proportional to its photosynthetic capacity, measured as the maxi-

Table I. *Effects of DCMU, DBMIB, and CCCP on Energy Storage in Far Red Light by Ulva and Porphyra*

The measuring light for *Porphyra* was 700 nm, 4.8 nm half-bandwidth, 23.4 μmol photons m^{-2} s^{-1} average intensity, modulated at 20 Hz. The measuring light for *Ulva* was 710 nm, 4.8 nm half-bandwidth, 10.7 μmol m^{-2} s^{-1} average intensity, modulated at 64 Hz. Nonmodulated white background light intensity was 1180 μmol photons m^{-2} s^{-1} (400–700 wavelength band). *Porphyra* in DCMU was exposed to 10 min of the nonmodulated white background light to induce increased ES (see the text). Similar induction of the other treatments did not increase ES.

Treatment	Energy Storage in Far Red Light	
	Porphyra	*Ulva*
	%	
No inhibitors	11.0	21.5
25 μM DCMU	20.0	21.4
100 μM DBMIB	6.4	12.8
100 μM CCCP	15.0	11.8

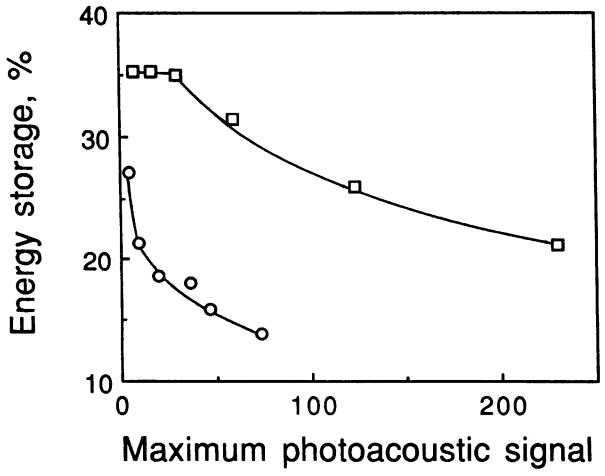

Figure 3. Energy storage *versus* maximum photoacoustic signal over a range of measuring light intensities in *Ulva*. The maximum photoacoustic signal is proportional to absorption of measuring light by the sample. Measuring lights used were 670 nm, 8.0 nm half-bandwidth (□) and 710 nm, 8.0 nm half-bandwidth (○). The maximum average intensities used for the 670 and 710 nm lights were 145.6 and 218.4 μmol photons m^{-2} s^{-1} respectively. The measuring beam was modulated at 64 Hz.

mum rate at which stable photochemical products are generated. The relative ES capacity of three algal species in the presence and absence of DCMU was determined by measuring ES over a broad range of light intensity and then multiplying the ES values observed by the intensity of incident measuring light. The resulting values of relative ES rate are plotted in Figure 5 *versus* the incident measuring light intensity to yield a curve that is analogous to the classical photosynthesis *versus* light intensity curve. The maximum ES rate values of these curves may be taken to be the ES capacity of the sample and are comparable between samples so long as absorption of incident light by the samples is the same.

In Figure 5, the absorption of the measuring light differed between the different algal species so that the relative energy storage capacities are not comparable between species. Within a species or sample, however, the relative capacities of energy storage in the presence and absence of DCMU may be compared, since the same measuring light was used for both. Thus, from Figure 5 it is possible to say that the DCMU-resistant energy storage capacity in *Anacystis* is 15.3% of the energy storage capacity in the absence of inhibitors. In *Ulva* and *Porphyra,* the energy storage capacity in DCMU is 3.5 and 3.8%, respectively, of energy storage capacity in the absence of inhibitors. As noted in "Materials and Methods," the ES measurements of Figure 5 were taken quickly to avoid any possible CO_2 limitation in the sample. Apparent CO_2 limitation of ES was readily observable in noninhibited samples if the measurements at high measuring light intensities were prolonged for more than a few minutes. In DCMU-treated samples, however, no such apparent CO_2 limitation was observed to occur.

The ES capacity in DCMU can be made to vary considerably with differing light treatments. These light-induced dynamics are seen in the photoacoustic signal traces shown in

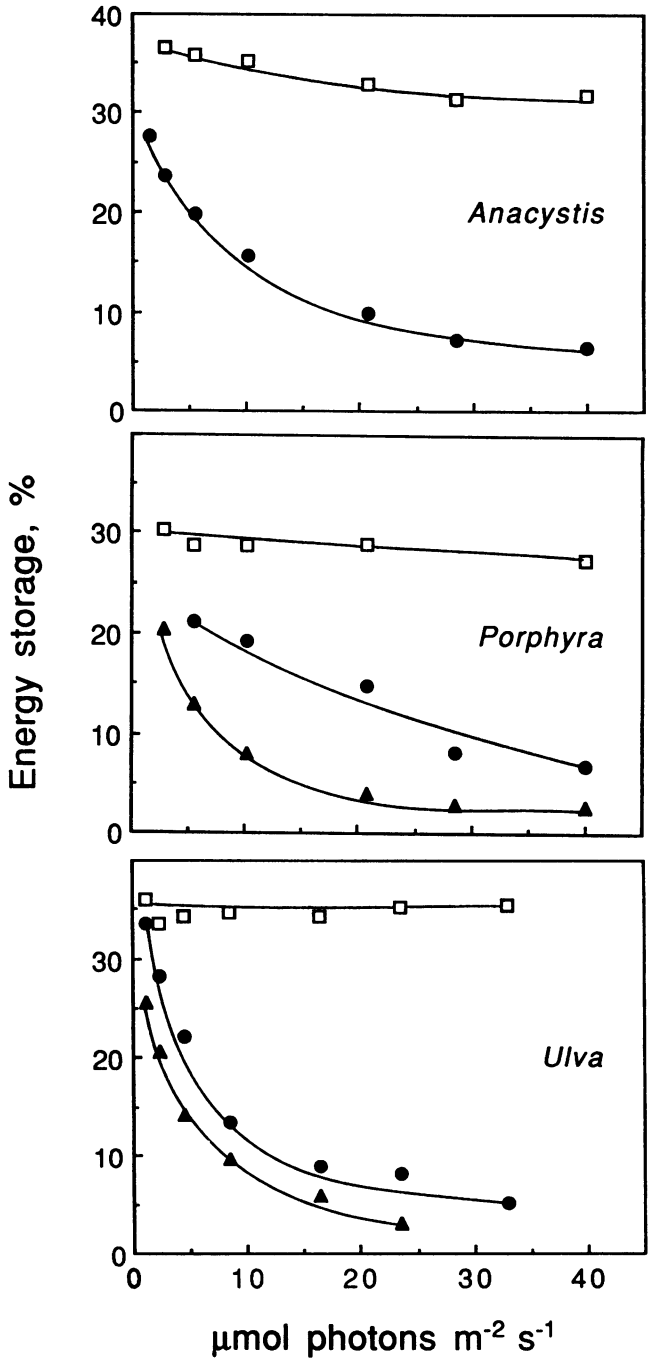

Figure 4. Energy storage *versus* the average intensity of the modulated measuring light in controls (□), samples treated with 25 μM DCMU (●), and samples treated with 100 μM DBMIB (▲). The measuring light was narrowband (4.8 nm half-bandwidth) centered at 670 nm for *Ulva* and centered at 620 nm for *Anacystis* and *Porphyra*. Continuous white background light was 1180 μmol photons m^{-2} s^{-1} (400–700 nm). Frequencies of measuring beam modulation were as described in Figure 1 for the different species.

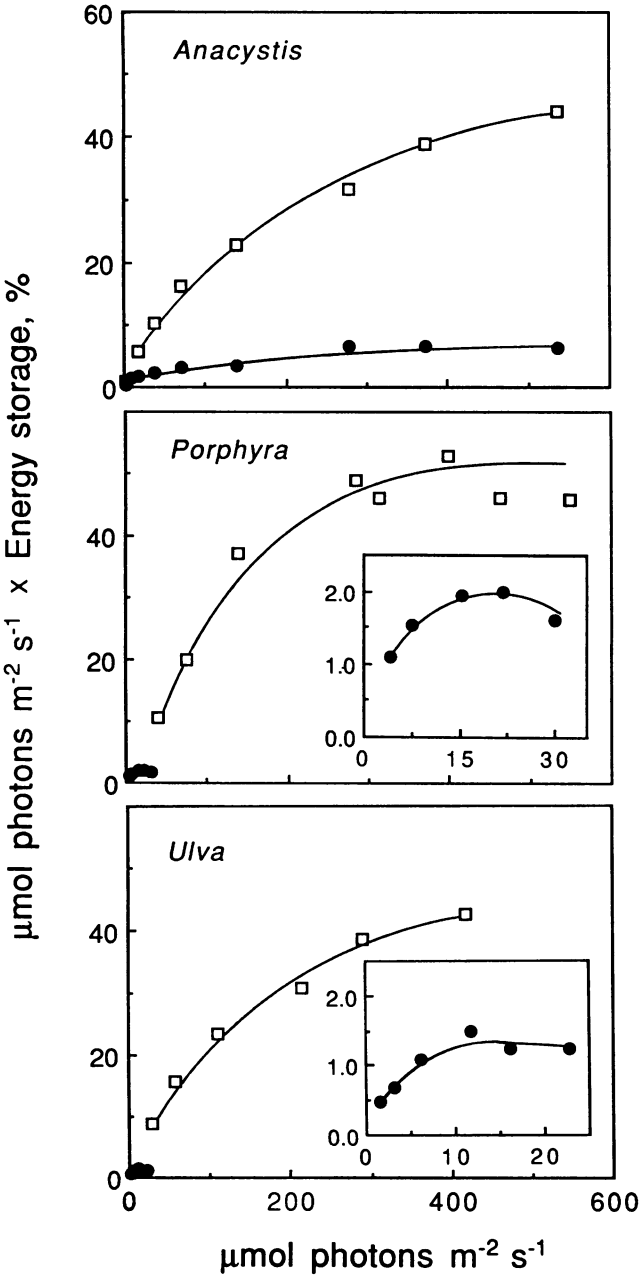

Figure 5. Relative energy storage rate *versus* average modulated measuring beam intensity in controls (□) and in samples treated with 25 μM DCMU (●). Relative ES rates were calculated as the measuring beam intensity multiplied by the ES observed at that intensity. Relative ES rates are thus proportional to the rates at which absorbed measuring light energy is stored in photochemical products. The measuring beam was broadband (19 nm half-bandwidth) centered at 620 nm for *Anacystis* and *Porphyra* and centered at 670 nm for *Ulva*. Nonmodulated white background light was 2000 μmol photons m^{-2} s^{-1} (400–700 nm). Frequencies of measuring beam modulation were as described in Figure 1 for the different species.

Figure 6. All three traces were made in 25 μM DCMU with a measuring light of 700 nm. The simplest dynamics were seen in *Ulva,* which showed a doubling of ES from an initial low value when the measuring light was first turned on to a final value achieved after 1 to 2 min in the measuring light. (This effect was seen in the trace as a gradual decline in the photoacoustic signal during the first 2 min of the measurement.) The addition of strong, nonmodulated background light had no effect on ES by *Ulva* in DCMU, even if the short exposures shown in Figure 6 were extended for 7 to 10 min. By contrast, strong, nonmodulated white background light produced a dramatic, reversible increase of energy storage in

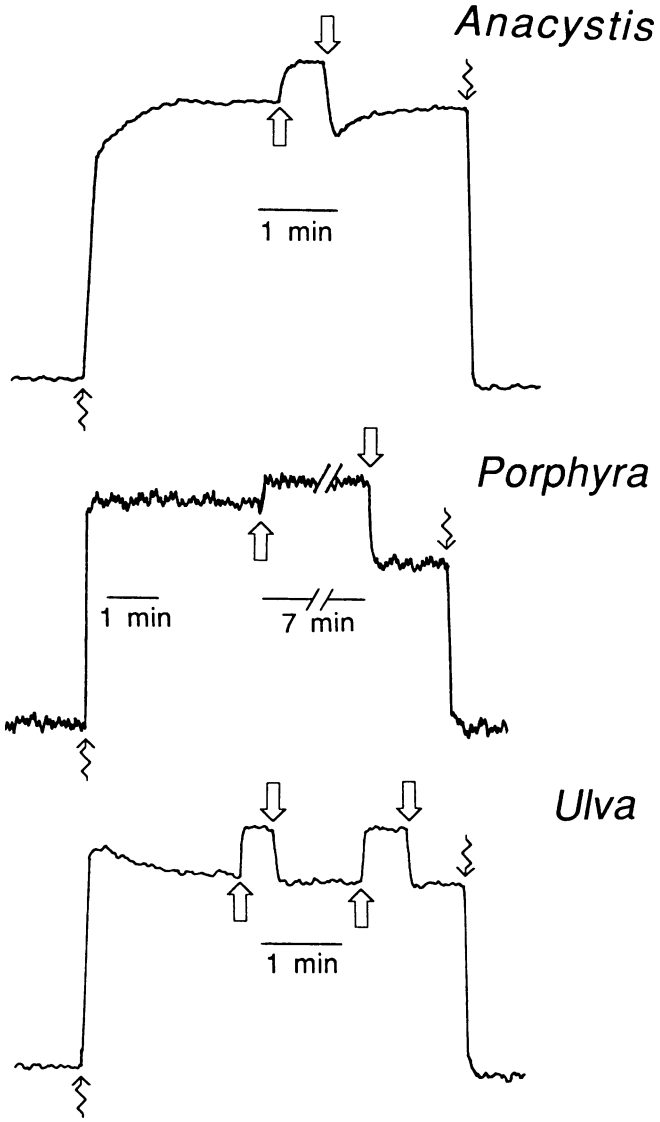

Figure 6. Photoacoustic signals in 25 μM DCMU with 700 nm modulated measuring light (4.8 nm half-bandwidth). Arrows are the same as in Figure 1. Average measuring beam intensities in μmol photons m^{-2} s^{-1}, were 11.7 for *Anacystis,* 13.5 for *Porphyra,* and 23.4 for *Ulva*. Nonmodulated white background light was 1180 μmol photons m^{-2} s^{-1} (400–700 nm). Frequencies of measuring beam modulation were as described in Figure 1 for the different species.

the presence of DCMU in both *Anacystis* and *Porphyra* (seen in the trace as a markedly lower photoacoustic signal following the white light exposure). In *Anacystis,* the induction and reversal of the increase in energy storage were both rapid, occurring in roughly 1 min. In *Porphyra,* both the induction and reversal of the increase in energy storage occurred on a much slower time scale than in *Anacystis.* Full induction of increased energy storage in *Porphyra* required exposure of 5 min or longer to strong, nonmodulated white background light while reversal in the measuring light alone (not shown) required more than 5 min. (It should be noted that, in all preceding data, ES measurements for *Porphyra* in DCMU were made with samples that were fully induced by strong, nonmodulated white light. No such improvement of ES by strong light occurred in DBMIB, CCCP, or in the absence of inhibitors.)

The trace in Figure 6 for *Anacystis* also shows a transient high energy storage immediately upon 700 nm illumination that decreased to a lower level (increase in the photoacoustic signal) within 1 min. This transient is not present in the 700 nm trace for the *Anacystis* of Figure 1 because the sample was insufficiently dark adapted.

DISCUSSION

Energy storage in far red light is most probably due to production of relatively long-lived photochemical products by means of cyclic electron flow through PSI (9, 18). This conclusion is supported by the observations that such energy storage occurred in far red wavelengths of light not absorbed by PSII (Figs. 1 and 2), that it was not inhibited by DCMU, and that it was inhibited by the plastoquinone antagonist DBMIB (Table I), which is known to inhibit cyclic electron flow around PSI (24). In the presence of DCMU, energy storage at all photosynthetically active wavelengths probably also occurs almost exclusively by means of cyclic electron flow through PSI, since no other energy-storing process leading to stable photochemical products is known to occur in DCMU. The actual photochemical products of cyclic electron flow through PSI that are detected photoacoustically are unknown though it is reasonable to suppose that ATP resulting from cyclic photophosphorylation accounts for most of the storage with some possible contribution of reduced intermediates in the cycle such as reduced ferredoxin. The inhibitory effect of CCCP on energy storage in far red light (Table I) supports the supposition that at least part of the energy storage is ATP synthesis, since CCCP is known to inhibit photophosphorylation by dissipating the *trans*-thylakoid proton gradient (15). Measurements of ES in DCMU or in far red light for *Porphyra* and *Sorghum* were made at measuring light modulation frequencies of 20 Hz, indicating that the observed photochemical products had a lifetime of at least 8 ms (11, 19).

It should be noted that the spectra of ES in DCMU of Figure 2 differ from the spectra in the absence of DCMU in that the ES values in DCMU are not maximal for the various wavelengths. As seen in Figures 3 and 4, energy storage in DCMU or in far red light begins to be light-saturated at very low measuring beam intensities and the light-limited range of maximal ES was not measurable in our apparatus. The intensity of the measuring light used in the spectra of Figure 2 was well within the maximal ES range of the ES *versus* intensity response for wavelengths absorbed by PSII in noninhibited samples, but it was not so for wavelengths absorbed exclusively by PSI or for any wavelength when the samples were treated with DCMU. Thus, the ES spectra in DCMU are at least partly the inverse of the absorption spectra of the sample, ES being low when absorbed measuring light is high. In both the presence and absence of DCMU, this effect contributes to the rise or peak in the far-red where absorption of the measuring light by the sample is low.

An interesting result seen in Figures 1 and 2 is that C_3-type higher plants, such as *Oxalis,* do not exhibit any measurable energy storage by cyclic electron flow through PSI when PSII is inactive. This result is contrary to experiments with preparations of thylakoids from C_3-type higher plants which clearly exhibit photophosphorylation driven by cyclic electron flow through PSI *in vitro* (2, 14). It is possible that some activity of PSII is required for cyclic electron flow to occur in C_3 higher plants. *In vitro* photophosphorylation induced by cyclic electron flow is typically enhanced by inhibition of PSII by DCMU or by irradiating PSI alone with far red light; this photophosphorylation is strongly inhibited, however, if the inactivation of PSII is absolute, as when PSI is irradiated alone in samples also treated with DCMU (2). It is thought that a few electrons provided by PSII are necessary to prime or 'poise' the PSI cycle and it is possible that in our experiments PSII was completely inactivated by 25 μM DCMU. All of the algal species in our experiments showed clear energy storage in DCMU and far red light (Figs. 2 and 6; Table I) but poising of the PSI cycle in these organisms could have been accomplished by electron supply to the plastoquinone pool from respiratory electron transport in the chloroplast (chlororespiration), which is known to occur in green algae and cyanobacteria (3, 23). In the case of C_4 plants, PSI-cyclic electron flow could be poised by electrons from malate pools (17).

Alternatively, it is possible that energy storage by cyclic electron flow through PSI simply does not occur in C_3 higher plants *in vivo* even though it is retained in the algae. An evolutionary rationale may be offered in support of this conclusion. Unlike higher plants, algae tend to have little capacity to store photosynthate because they typically have no specialized storage tissues. Thus, in the algae, any special needs for ATP by processes such as nutrient uptake or responses to stress requiring protein synthesis must be met directly by photophosphorylation supported by cyclic electron flow while higher plants may rely on metabolism of stored photosynthate to provide extra ATP.

From Figures 4 and 5 it is clear that, in algae, the capacity for ES by cyclic electron flow through PSI when PSII is inactive is a small fraction of the capacity for energy storage of both PSI and PSII operating together. Our value of 15.3% for this fraction in *Anacystis* (Fig. 5) compares well with the results of Myers (20) for other cyanobacteria. We would not agree with Myers, however, that this amount of photophosphorylation is physiologically insignificant. Even small amounts of ATP produced by cyclic electron flow through PSI may be important for repair of stress-damaged PSII units,

as proposed by Canaani *et al.* (9). As an example, photoinhibition repair in *Phaseolus* is measurably improved by recovery in relatively low levels of light as opposed to darkness (13) suggesting that even low levels of photosynthetic activity are helpful. The limiting factor to ES capacity by PSI cyclic flow appears to be turnover of some step in the cycle rather than lack of a substrate such as ADP, since DBMIB reduces ES capacity. The inhibition of PSI-cyclic ES by DBMIB is also interesting in that it is incomplete. It is possible that 100 μM DBMIB is insufficient to completely inhibit cyclic electron flow around PSI. Alternatively, cyclic electron flow through PSI may operate by two pathways, as shown by Hosler and Yocum (14), one of which may not be sensitive to DBMIB.

Light-induced dynamics of ES capacity in 700 nm measuring light and DCMU were evident in the three species of algae that were examined. These dynamics cannot be interpreted without further study but perhaps the dynamics seen in *Ulva* can be most easily explained as simple light activation of photophosphorylation, perhaps by development a *trans*-thylakoid proton gradient by cyclic electron flow through PSI. The lack of an additional effect on ES by strong nonmodulated white background light may result because the rate of PSI-cyclic flow is already at a maximum and additional light does not increase the proton gradient. The dynamics of ES capacity in 700 nm light and DCMU exhibited by *Anacystis* and *Porphyra* are more difficult to account for. The improvement of ES capacity in *Porphyra* by strong nonmodulated white light has previously been suggested to indicate a functional heterogeneity of PSI units (18). It was suggested for red algae, which typically have a PSII to PSI ratio of less than 1, that PSI units are of two types: (a) those that accept electrons from PSII and do not normally participate in cyclic electron flow, and (b) those that participate only in cyclic electron flow. With exposure to strong white light in the presence of DCMU, PSI units normally engaged only in linear electron flow from PSII are altered so that they can participate in cyclic electron flow, increasing ES capacity by PSI-cyclic flow. Some variation of this same hypothesis might also hold for the similar but much faster dynamics of *Anacystis*.

In summary, energy storage by cyclic electron flow through PSI, presumably reflecting photophosphorylation, is readily measurable *in vivo* using the photoacoustic technique. Measurements of this type made on a wide variety of photosynthetic organisms indicate that cyclic photophosphorylation *in vivo* occurs in all with the possible exception of higher plants using the C_3 carbon fixation pathway. The energy storage capacity of cyclic photophosphorylation alone appears to be small by comparison to the capacity of energy storage by linear and cyclic electron flow combined but may be significant under conditions when PSII is inhibited or when an increased proportion of ATP from photosynthesis is needed, particularly in algae and cyanobacteria. Light-induced dynamics of energy storage by cyclic electron flow *in vivo* are apparent and demonstrate its regulation under changing environmental conditions. It is hoped that additional study utilizing the photoacoustic technique will better define the role of cyclic electron flow in oxygen-evolving photosynthetic organisms.

ACKNOWLEDGEMENTS

The authors gratefully acknowledge the assistance of Mr. Brian Welsh who constructed the photoacoustic cell. Microphones for the photoacoustic cell were graciously provided by Mr. Michael Abry of Knowles Electronics Inc., Franklin Park, IL.

LITERATURE CITED

1. **Arnon DI, Chain RK** (1975) Regulation of ferredoxin-catalyzed photosynthetic phosphorylations. Proc Natl Acad Sci USA **72:** 4961–4965
2. **Arnon DI** (1977) Photosynthesis 1950–75: changing concepts and perspectives. *In* A Trebst, M Avron, eds, Encyclopedia of Plant Physiology, Vol 5. Photosynthesis I, Photosynthetic electron transport and photophosphorylation. Springer-Verlag, Berlin, pp 7–56
3. **Bennoun P** (1982) Evidence for a respiratory chain in the chloroplast. Proc Natl Acad Sci USA **79:** 4352–4356
4. **Blinks LR** (1964) Accessory pigments and photosynthesis. *In* AC Giese, ed, Photophysiology I. Academic Press, New York, pp 199–221
5. **Bults G, Horwitz BA, Malkin S, Cahen D** (1982) Photoacoustic measurements of photosynthetic activities in whole leaves: photochemistry and gas exchange. Biochim Biophys Acta **679:** 452–465
6. **Buschmann C, Prehn H, Lichtenthaler H** (1984) Photoacoustic spectroscopy (PAS) and its application in photosynthesis research. Photosynth Res **5:** 29–46
7. **Canaani O** (1986) Photoacoustic detection of oxygen evolution and state 1-state 2 transitions in cyanobacteria. Biochim Biophys Acta **852:** 74–80
8. **Canaani O** (1990) The role of cyclic electron flow around photosystem I and excitation energy transfer distribution between the photosystems upon acclimation to high ionic stress in *Dunaliella salina*. Photochem Photobiol **52:** 591–599
9. **Canaani O, Schuster G, Ohad I** (1989) Photoinhibition in *Chlamydomonas reinhardtii:* effect on state transitions, intersystem energy distribution, and Photosystem I cyclic electron flow. Photosynth Res **20:** 129–146
10. **Carpentier R, LaRue B, LeBlanc RM** (1984) Photoacoustic spectroscopy of *Anacystis nidulans*. III. Detection of photosynthetic activities. Arch Biochem Biophys **228:** 534–543
11. **Carpentier R, Nakatani H, LeBlanc RM** (1985) Photoacoustic detection of energy conversion in a Photosystem II submembrane preparation from spinach. Biochim Biophys Acta **808:** 470–473
12. **Gimmler H** (1977) Photophosphorylation *in vivo*. *In* A Trebst, M Avron, eds, Encyclopedia of Plant Physiology, Vol 5. Photosynthesis I, Photosynthetic electron transport and photophosphorylation. Springer-Verlag, Berlin, pp 448–472
13. **Greer DH, Berry JA, Björkman O** (1986) Photoinhibition of photosynthesis in intact bean leaves: role of light and temperature, and requirement for chloroplast-protein synthesis during recovery. Planta **168:** 253–260
14. **Hosler JP, Yocum CF** (1985) Evidence for two cyclic phosphorylation reactions concurrent with ferredoxin-catalyzed noncyclic electron transport. Biochim Biophys Acta **808:** 21–31
15. **Izawa S, Good NE** (1972) Inhibition of photosynthetic electron transport and photophosphorylation. Methods Enzymol **24:** 355–377
16. **Lasser-Ross N, Malkin S, Cahen D** (1980) Photoacoustic detection of photosynthetic activities in isolated broken chloroplasts. Biochim Biophys Acta **593:** 330–341
17. **Leegood RC, Crowther D, Walker DA, Hind G** (1983) Energetics of photosynthesis in *Zea mays*. I. Studies of the flash-induced electrochromic shift and fluorescence induction in bundle sheath cells. Biochim Biophys Acta **722:** 116–126
18. **Malkin S, Herbert SK, Fork DC** (1990) Light distribution, transfer and utilization in the marine red alga *Porphyra perforata* from photoacoustic energy storage measurements. Biochim Biophys Acta **1016:** 177–189

19. **Malkin S, Lasser-Ross N, Bults G, Cahen D** (1981) Photoacoustic spectroscopy in Photosynthesis. *In* G. Akoyunoglou, ed, Photosynthesis, Vol 3. Structure and Molecular Organisation of the Photosynthetic Apparatus. Balaban International Science Services, Philadelphia, pp 1031–1042
20. **Myers J** (1987) Is there significant cyclic electron flow around photoreaction I in cyanobacteria? Photosynth Res **14:** 55–69
21. **Osmond CB** (1974) Carbon reduction and Photosystem II deficiency in leaves of C_4 plants. Aust J Plant Physiol **1:** 41–50
22. **Poulet P, Cahen D, Malkin S** (1983) Photoacoustic detection of photosynthetic oxygen evolution from leaves. Quantitative analysis by phase and amplitude measurements. Biochim Biophys Acta **724:** 433–446
23. **Scherer S, Almon H, Böger P** (1988) Interaction of photosynthesis, respiration, and nitrogen fixation in cyanobacteria. Photosynth Res **15:** 95–114
24. **Trebst A** (1980) Inhibitors in electron flow: tools for the functional and structural localization of carriers and energy conservation sites. Methods Enzymol **69:** 675–715